

1 **PERFORMANCE EVALUATION OF DRYING SHRINKAGE AND DURABILITY IN**
2 **PAVEMENT QUALITY CONCRETE WITH RECYCLED AGGREGATE, GGBS AND I-**
3 **CRETE**

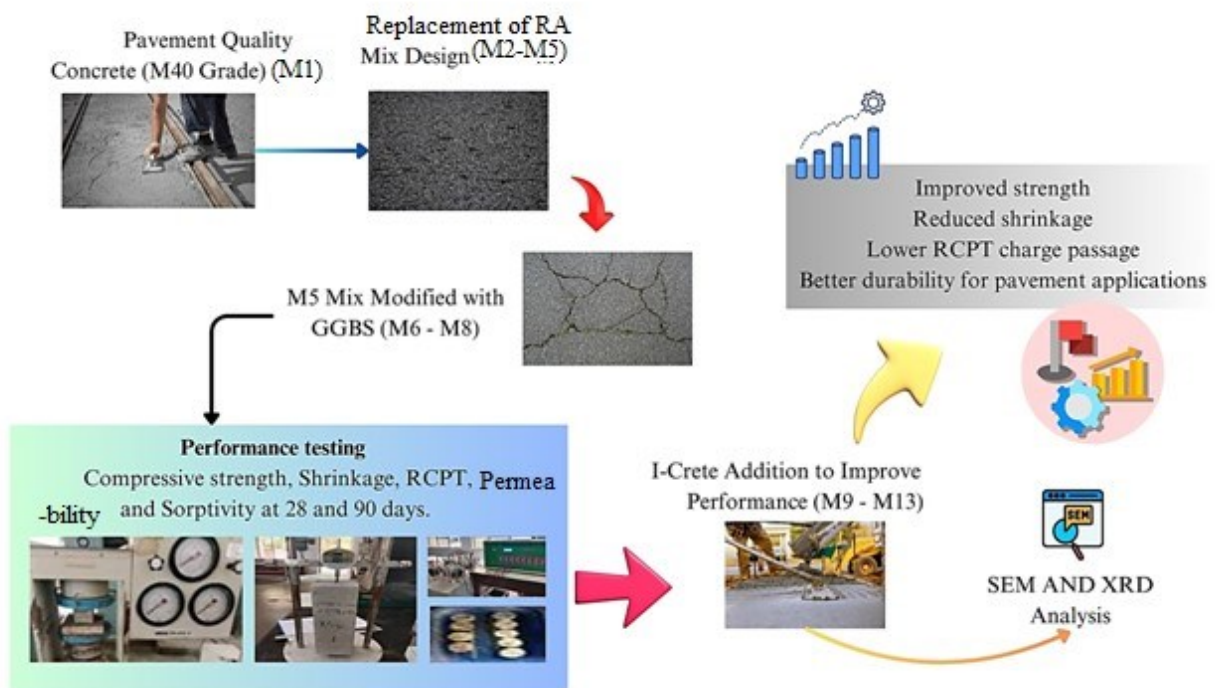
4 **B. Chittibabu^{1,*} and Prof. K. Durga Rani²**

5 ¹Research Scholar, Civil Engineering Department, Andhra university, Visakhapatnam, Andhra
6 Pradesh, India.

7 ²Professor, Civil Engineering Department, Andhra university, Visakhapatnam, Andhra Pradesh,
8 India.

9 *Corresponding author: B. Chittibabu, E-mail: bchittibabu.rs@andhrauniversity.edu.in*

10
11 **GRAPHICAL ABSTRACT**



12
13 **ABSTRACT**

14 The study examines replacement of Natural Aggregates (NA) with Recycled Aggregate (RA) in
15 Pavement Quality Concrete (PQC) M40 grade (M1) with 25%, 50%, 75% and 100% RA replacing
16 NA in M2, M3, M4 and M5 mixes. The compressive strength decreases with higher RA, but all

17 mixes reach the target strength at 28 and 90 days. M5 was tested by adding Ground Granulated
18 Blast furnace Slag (GGBS) in increments of 5% to 15% in M6, M7 and M8 to reduce the cement
19 content. The main performance parameters include compressive strength, drying shrinkage, water
20 penetration, Rapid Chloride Permeability Test (RCPT) at 28 and 90 days and sorptivity at 28 days.
21 M5 reduced compressive strength but increased drying shrinkage, sorptivity, penetration depth and
22 RCPT charge passage. Increasing the GGBS by 10% in M7 improved the strength, while increasing
23 the GGBS by 15% in M8 decreased the strength compared to M1 and M5. To address strength
24 degradation, the study incorporated 2% I-Crete along with GGBS in 5% increments from 15% to
25 35% in M9 to M13 mixes. M11 mix (2% I-Crete, 25% GGBS) showed better strength, reduced
26 shrinkage and lower RCPT charge, ensuring better durability for SEM and XRD pavement
27 applications.

28 **Keywords:** RA, Drying shrinkage, GGBS, I-Crete, RCPT, Sorptivity, Penetration depth.

29 **1. Introduction**

30 The swift growth of global economies and construction activities has raised concern about the
31 degradation of natural resources and management of concrete waste. The construction sector, a
32 major contributor to environmental deterioration, consumes a significant amount of natural
33 resources and generates around 10 billion tons of construction debris worldwide each year, around
34 thirty percent of the entire amount of solid waste (Mao et al. 2021; Singh & Singh., 2021). The
35 increasing environmental impact underscores the need for sustainable practices, such as
36 incorporating RA into concrete mixtures. By reducing total natural demand, RA has major positive
37 impacts on the environment, economy and society (Silva et al., 2019; Tam et al., 2018).

38 This research continues to explore the optimal use of RA in highway pavement concrete,
39 emphasizing its role in developing sustainable construction practices.

40 GGBS, a by-product of the iron and steel producing process, has been widely used as a
41 Supplementary Cementitious Material (SCM) in concrete construction due to its environmental

42 benefits and its ability to improve concrete durability (Lim.y et al., 2021). Studies have
43 demonstrated that partially replacing Portland cement with GGBS effectively reduces the carbon
44 footprint of the construction industry while supporting sustainable practices (Hwang .J et al., 2013).
45 The incorporation of GGBS, along with other SCMs. This includes fly ash and silica fume, to
46 significantly improve both the mechanical properties and durability of concrete. Replacing 30% of
47 cement with GGBS and 50% with coal fly ash has resulted in marked improvements in concrete
48 performance (Wang et al., 2021). The mechanical properties of the concrete mixture are lower at the
49 early stage (7 days) but reach maximum strength at a later stage (90 days) due to the lower strength
50 heat of hydration. The finer GGBS particles enhance the concrete's microstructure and pore
51 distribution, leading to reduced shrinkage, increased durability, and improved stability by making
52 the concrete denser (Zhang et al., 2023; Hwang et al., 2013).

53 I-Crete, a high-quality mineral additive compliant with ASTM C1797 and IS 2645, is highly
54 reactive and has a well-regulated particle size, with less than 10% retained on a 45-micron sieve.

55 The present phase of research focuses on optimizing the use of GGBS in highway pavement
56 concrete, with an emphasis on its role in advancing sustainable construction practices. This study
57 analyze the impact of GGBS on the mechanical properties and durability of concrete, particularly
58 in the context of highway pavements. It investigates the optimal replacement levels of GGBS to
59 achieve maximum strength and durability, while also assessing the effects on shrinkage and stability
60 due to alterations in concrete's microstructure and pore distribution. The goal is to identify the most
61 effective use of GGBS to improving the performance and sustainability of highway concrete
62 pavement..

63 The study investigates the optimal use of RA in PQC. It examines the effects of substituting NA
64 with RA and further replacing cement with GGBS, in addition to incorporating I-Crete. The study
65 aims to determine whether these substitutions help achieve the target strength and enhance concrete
66 performance. By varying percentages of RA, GGBS, and I-Crete, the research evaluates their

67 impact on concrete strength and durability at both early and later stages. This approach seeks to
68 provide a sustainable solution for concrete pavements, improving long-term durability and
69 environmental benefits while addressing the increasing demand for recycled materials in the
70 industry.

71 ***1.1 Research Significance***

72 The study advances sustainable PQC by exploring the maximum replacement of NA with RA. It
73 addresses a key gap in understanding RA application in pavement construction. By utilizing GGBS
74 as a partial cement replacement and incorporating I-Crete.

75 The study aims to improve the compressive strength and durability of PQC in this paper, the key
76 parameters examined include compressive strength, drying shrinkage, durability, chloride ion
77 diffusion resistance, sorptivity, and water penetration. Parameter of findings provides insights into
78 reducing the carbon footprint of PQC, promoting environmental sustainability, and supporting the
79 use of recycled materials in pavement construction.

80 **2. Materials and mix Proportions**

81 *2.1. Data collection*

82 In this research, RA with a nominal size of 20-10 mm was sourced from Construction and
83 demolition waste plant, facility in Hyderabad, Telangana. River sand conforming to Zone-II as per
84 IS 383-2016 and OPC 53 grade cement from Visakhapatnam were used. In the mix Additionally,
85 GGBS and I-Crete were procured from Visakhapatnam and Chennai, respectively. Potable water
86 and CONPLAST SP 430 chemical admixture were used as per IS 456-2000.

87 Based on the trial studies performed with different dosages of I-crete, the outcomes indicated that
88 the optimum results are observed with 2% of I-Crete. Based on the test outcomes of trial studies,
89 2% I-crete was chosen as optimum percentage.

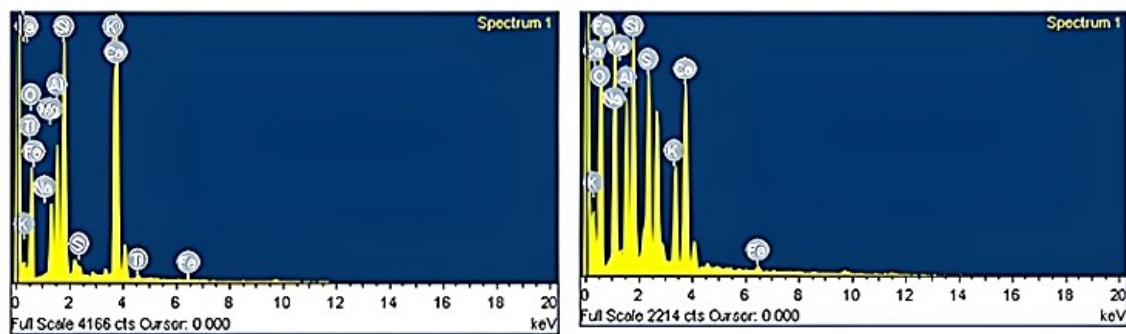


Figure 1 (a) GGBS spectrum (b) I-Crete Spectrum

2.2. Data measurement

The study adhered to standard testing protocols for durability parameters, including sorptivity, RCPT, and water penetration. Sorptivity was measured as per ASTM C1585, which quantifies the absorption of water by concrete over time. RCPT was conducted following ASTM C1202, which measures the charge passed through concrete as a proxy for chloride ion permeability. For water penetration depth, the study followed IS 516 : Part 2 : Sec 1 , ensuring consistency and accuracy in the evaluation of the concrete's resistance to water ingress, critical for assessing durability in pavement applications.

2.3. Physical Characterization

Physical characteristics of the materials were as follows: NA had a specific gravity of 2.84, bulk density (Compacted) of 1800 kg/m³, aggregate impact value of 18.96%, and aggregate crushing value of 18.01%. In contrast, RA exhibited a lower specific gravity of 2.60, bulk density (Compacted) of 1600 kg/m³, and higher impact and crushing values of 23.40% and 25.47%, respectively. Cement had a specific gravity of 3.15 and a standard consistency of 30%, GGBS had a specific gravity of 2.90 and a consistency of 32%, as shown in the EDAX spectrum in Figure (a). I-Crete had a specific gravity of 2.43 and a consistency of 22%, as illustrated by the EDAX spectrum in Figure 1(b). RA having lower Physical and mechanical characteristics as compared to NA, RA complies with IS 383-2016 and MORTH standards and was used under Saturated Surface Dry (SSD) conditions. The inclusion of I-Crete as an additive in the study plays a crucial role in enhancing the durability of PQC, particularly when replacing higher proportions of natural

112 aggregates with RA. Unlike traditional additives, I-Crete has been shown to reduce the detrimental
 113 effects of RA on compressive strength and drying shrinkage. By incorporating I-Crete, especially in
 114 mixes with higher RA content, the study found improvements in strength retention and reduction in
 115 shrinkage, which are essential for enhancing the long-term durability of concrete structures,
 116 particularly in pavement applications.

117 **2.4 Mix Proportions**

118 The mix design for M40 grade concrete followed IRC-44-2017, IRC-15-2017, and IS 10262-2019
 119 standards. RA was used in a 60:40 ratio, with 60% of the coarse aggregate (20-10 mm) replaced by
 120 natural aggregate at 25% intervals, and the remaining 40% consisting of 10 mm natural aggregate.
 121 GGBS was used at 5% intervals, replacing 5-35% of OPC, and 2% I-Crete was added to improve
 122 bonding in PQC. All mix notations as shown in Table.1

123

124

Table.1 Mix notations

Mix Id's	Mix notations
MNAC	M1
MRCA-25	M2
MRCA-50	M3
MRCA-75	M4
MRCA-100	M5
MRCA-100+5%GGBS	M6
MRCA-100+10%GGBS	M7
MRCA-100+15%GGBS	M8
MRCA-100+15%GGBS+2I	M9
MRCA-100+20%GGBS+2I	M10
MRCA-100+25%GGBS+2I	M11

MRCA-100+30%GGBS+2I	M12
MRCA-100+35%GGBS+2I	M13

125 *Note: MNAC: Mix Notation of Natural aggregate Concrete, MRCA: Mix of Recycled Concrete*
 126 *Aggregate, GGBS: Ground Granulated Blast Furnace Slag, RA=Recycled Aggregate,*
 127 *SCM=Supplementary Cementitious Material, I=I-crete (2%)*

128 **2.5 Studies on Hardened Concrete**

129 Concrete compressive strength was measured using standard 100 x 100 x 100 mm cubes in
 130 accordance with IS 516: Part 1: Section 1: 2021. Fig.2 shows the experimental setup. Drying
 131 shrinkage is tested by IS 516 (Part 6): 2020, micrometer gauge or dial gauge to 0.001 mm. Samples
 132 were prepared with mould dimensions of 75 x 75 x 300 mm and a vibrating table operating at
 133 minimum 40 Hz (as per IS 2514) was used for filling.

134



135

136 **Figure 2** Test setup for the Compressive strength

137 At least three samples were evaluated and the shrinkage was estimated as a percentage of strain.

138 Fig. 3 illustrates the experimental setup.



Figure 3 Test setup for Drying Shrinkage

139

140

141

142 Sorptivity was tested using disc specimen of 100 ± 6 mm diameter and 50 ± 3 mm depth, according to
 143 ASTM C1585-04. After oven-drying, the samples were partially submerged in water and their mass
 144 was measured regularly for 7 days to measure water absorption. Fig.4 shows the experimental
 145 setup. RCPT (ASTM C1202-12) used cylindrical specimens with 100 mm diameter and 50 ± 3 mm
 146 depth aged 28 and 90 days (according to C192/C192M).

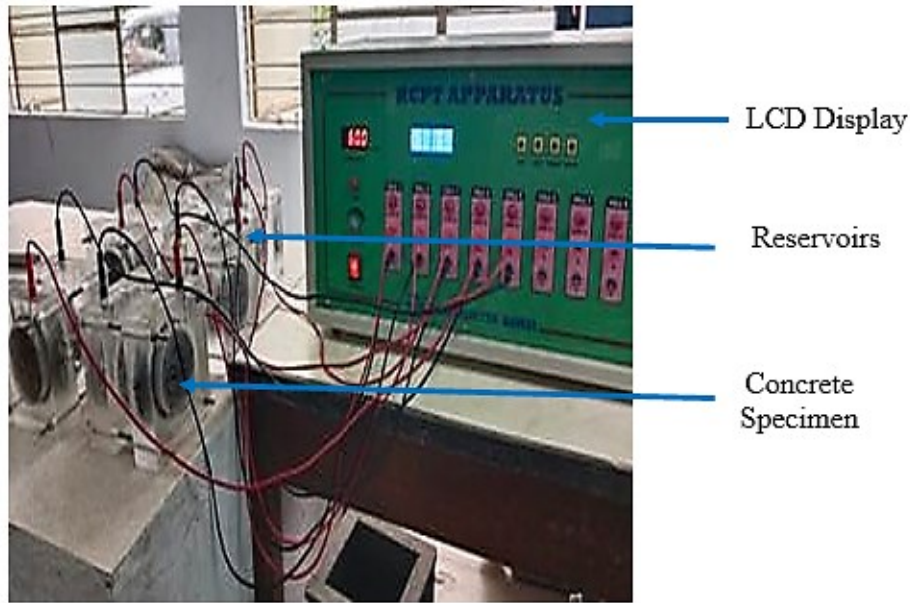


147

148

Figure 4 Test setup for Sorptivity

149 The samples were sealed with low- or high-viscosity sealants and the electrical conductivity was
150 measured at 60 V over a period of 6 hours. Figure5 shows the experimental setup. Water
151 penetration depth was tested as per IS 516 (Part 2/Sec 1): 2018 using cylindrical specimen with 100
152 mm diameter and 100 mm depth.



153

Figure 5 Test setup for Rapid Chloride Permeability Test

155 The sample was held under a water pressure of 500 ± 50 kPa for 72 ± 2 hours, the sample was split
156 with the experimental setup shown in Figure 6. and the penetration depth was measured.



157

Figure 6 Test setup for Depth of penetration of water

158

159 3. Results and Discussion

159

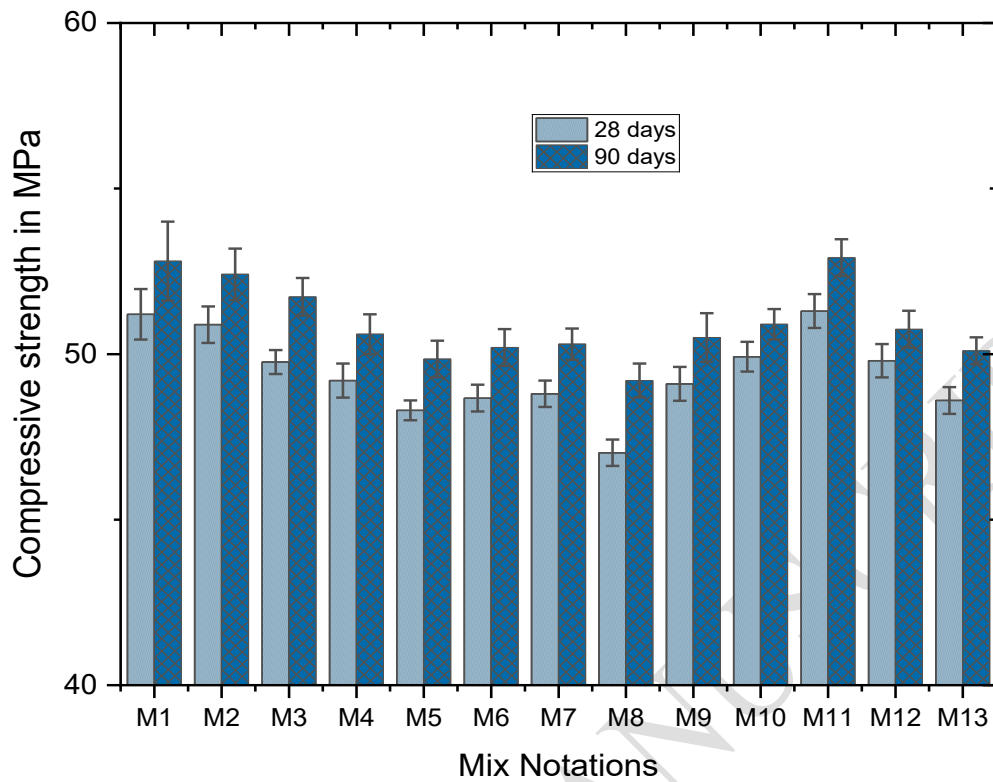
160 3.1. Compressive strength

160

161 The compressive strength of concrete diminishes as natural aggregates (NA) are progressively
162 replaced by recycled aggregates (RA) in 25% increments, up to 100%, as observed in the control
163 mix (M1) through M5. Specifically, compressive strength at 28 days decreased from 51.20 MPa to
164 48.30 MPa, and at 90 days from 52.81 MPa to 49.80 MPa, largely due to the weaker interfacial
165 transition zone (ITZ), higher porosity, and reduced mechanical properties of RA compared to NA
166 (Jindal & Ransinchung, 2018; Wang et al., 2021; IRC:121-2017; Kou et al., 2011). However, all
167 RA-replaced mixes still met the strength criteria set by IRC 58:2017 and IRC-44:2017. The study
168 further analyzed the impact of ground granulated blast-furnace slag (GGBS) on mixes with 100%
169 RA, where GGBS replacement of cement in 5–35% increments resulted in a maximum compressive
170 strength reduction of 4.68% at 28 days and 4.75% at 90 days in the M7 mix. Improved strength in
171 M7 over M5 is attributed to GGBS's fine particles and enhanced C-S-H gel formation (Hwang et
172 al., 2013; Kou et al., 2011; Sharma et al., 2021). In mixes with higher GGBS content, such as M6,
173 reduced early-age strength and delayed pozzolanic reactions led to a decline in compressive
174 strength (Kumar et al., 2023; Sharma et al., 2021). Notably, mix M11, with 25% GGBS and 2% I-
175 Crete, demonstrated improved compressive strengths of 51.30 MPa and 52.91 MPa at 28 and 90
176 days, respectively, I-Crete's role in promoting hydration and enhancing the concrete's
177 microstructure. For visual reference, these results are depicted in Figure 7.

178 The selection of specific Recycled Aggregate (RA) replacement percentages, ranging from 25% to
179 100%, was based on evaluating the trade-offs between maintaining the compressive strength of
180 Pavement Quality Concrete (PQC) while utilizing RA for sustainable construction. The impact of
181 RA on compressive strength was observed to decrease as RA content increased. However, all mixes
182 achieved the target strength at 28 and 90 days, demonstrating the feasibility of higher RA usage.
183 The choice of these percentages allows a balanced approach to optimizing the use of RA without
184 compromising on performance, while offering a solution to reduce reliance on natural aggregates.

185



186

187 **Figure 7** Variation of compressive strength Vs Mix notations for 28 and 90 days curing period

188 To support the compressive strength results, statistical analysis such as standard deviation and
 189 coefficient of variation can provide insights into the variability of strength across different mixes.

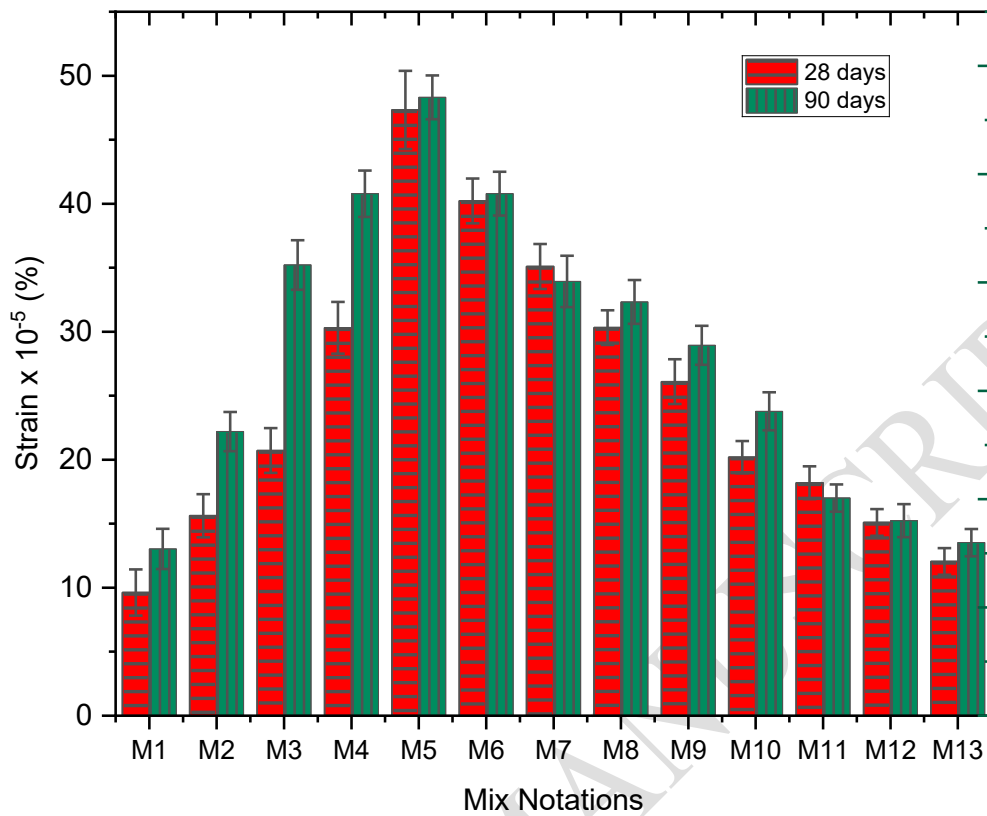
190 For example, while the compressive strength decreases with higher RA content (M5), the statistical
 191 data confirms that all mixes, including those with 100% RA, reach the target strength at 28 and 90
 192 days. The analysis demonstrates the consistency of the results and supports the feasibility of using
 193 RA up to 100% in PQC without compromising structural integrity.

194 *3.2 Drying shrinkage*

195 The substitute of NA with RA in the control mix (M1) led to increased drying shrinkage.
 196 Specifically, when Compared to M1 mix, M5 mix showed approximately 4.92 times higher strain
 197 levels after 28 days and 3.71 times higher strain levels at 90 days. This substantial increase in strain
 198 for the M5 mix is attributed to the utilize of RA, as Drying shrinkage increases with the replacement

199 of RA due to its higher porosity and weaker ITZ, which lead to greater moisture loss and internal
200 voids. (Duan and Poon, 2014; Mao et al., 2021; Yu.Y et al., 2021).

201 For M7 mix, strain values were approximately 3.64 and 2.60 times higher than M1 mix at 28 and
202 90 days, accordingly. Although the M7 mix showed increased drying shrinkage compared to the M1
203 mix, it was lower than that of the M5 mix. Adding GGBS to the mix decreases drying shrinkage by
204 improving the pore structure and reducing porosity through its pozzolanic reaction, which leads to a
205 denser matrix (Kumar and Mishra., 2022;Zhag.W et al., 2015;Mao et al., 2021). M11 mixture
206 exhibited 1.89 times greater strain value at 28 days and 1.31 times greater at 90 days than M1
207 mixture. The M11 mix showed the least increase in strain compared to the M1 mix, indicating more
208 stable performance over time. As RA content increases, the shrinkage also increases, as observed in
209 M5. The higher absorption capacity of RA leads to more significant volume changes during drying,
210 which results in increased drying shrinkage. This behavior examines the need for additives like
211 GGBS and I-Crete to mitigate the adverse effects of RA on shrinkage and enhance the long-term
212 stability of the concrete. This result highlights the effect of adding I-Crete, It reduces porosity and
213 improves the microstructure of concrete, and strengthens the ITZ, thereby reducing drying
214 shrinkage strain. The results are shown in Figure 8. GGBS and I-Crete work synergistically to
215 counteract the reduction in compressive strength with higher RA content by improving the
216 microstructure and reducing the effects of porosity. GGBS, as a SCM, enhances the hydration
217 process, improving the strength and durability of the concrete, while I-Crete enhances the bonding
218 between particles and reduces shrinkage. In the M9 to M13 mixes, the combination of 2% I-Crete
219 and GGBS in varying proportions effectively mitigated the strength loss observed with high RA
220 content, particularly in M11 (2% I-Crete, 25% GGBS), which showed improved strength and
221 reduced shrinkage



222

223 **Figure 8** Variation of Drying shrinkage (Strain in %) Vs Mix notations for 28 and 90 days curing
 224 period

225 The drying shrinkage behavior of each mix was compared to similar studies in the field of pavement
 226 concrete with RA. Studies have shown that higher RA content typically results in increased
 227 shrinkage due to the higher water absorption and porous nature of RA. The drying shrinkage
 228 observed in the M5 mix (100% RA) aligns with these findings, demonstrating that although higher
 229 RA content may improve sustainability, it introduces challenges in shrinkage, which must be
 230 mitigated with appropriate additives like GGBS and I-Crete to achieve better performance.

231 3.3 The Rapid Chloride Permeability Test (RCPT)

232 Rapid Chloride Permeability Test (RCPT) and Water penetration values were measured using
 233 standard testing procedures outlined by ASTM : C1202. and IS:516:part2:sec1 codes. The water
 234 penetration depth was evaluated by placing the concrete samples under a consistent water pressure

235 for a specified period, The depth of water penetration into the concrete specimens under pressure
236 was measured. The RCPT was performed by applying a constant 60V voltage across 100 mm
237 diameter and 50 mm thick concrete specimens to measure the charge passed, which indicates
238 permeability and chloride ion penetration resistance. Initial absorption was measured every half
239 hour for up to six hours, and secondary absorption was measured every 24 hours for up to eight
240 days. These tests were performed on all mixes at 28 and 90 days to evaluate the durability and
241 potential for corrosion in different mixes.

242 As RA was incorporated in the M1 mix, the overall charge passed increased. However, all mixes
243 M1 through M13 had charge passage levels within acceptable limits per ASTM C1202-12 for 28
244 and 90 days of curing. In mix M5, RCPT charge passes increased by 97.37% and 89.21%
245 compared to M1 mix at 28 and 90 days, respectively. RA increases porosity because of the mortar
246 debris on its surface, resulting in higher RCPT charge passage. This in turn, creates voids in the
247 concrete and weakens its resistance to chloride diffusion when subjected to an electrical charge (Jun
248 Phil Hwang et al., 2013; Wang.B et al., 2021).

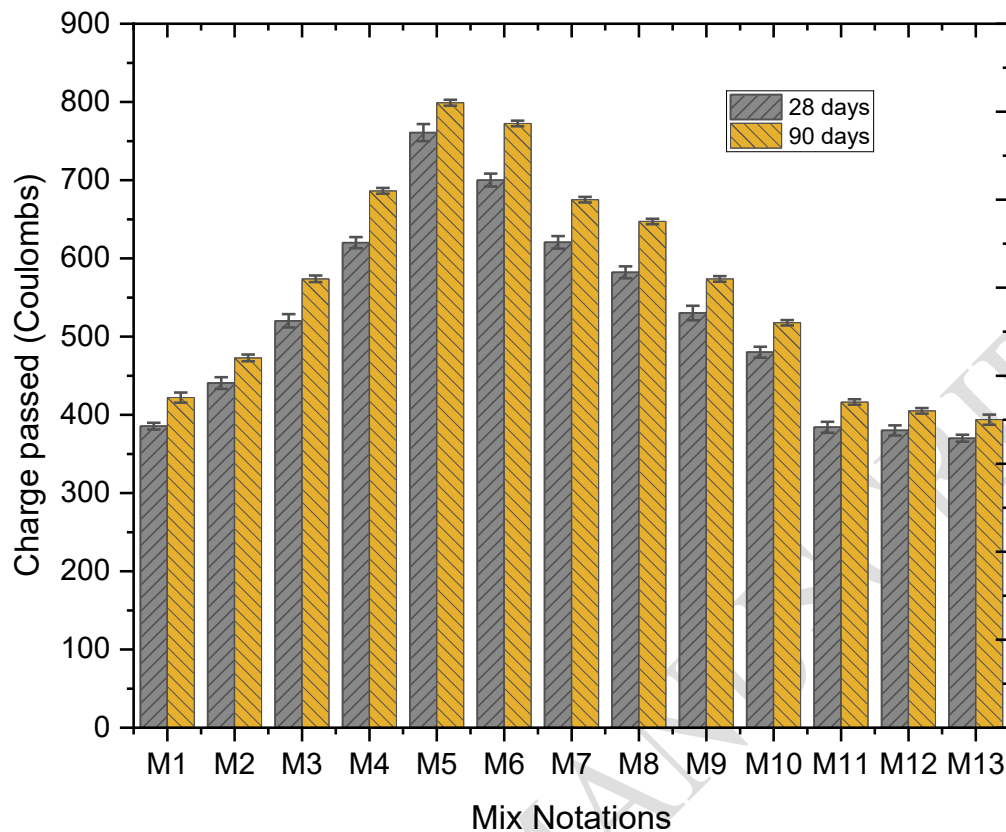


Figure 9 Variation of Charge passed Vs Mix notations for 28 and 90 days curing period

249

250

251 For M7 mix, charge passage increased by 60.95% and 59.89% at 28 and 90 days compared to M1.

252 However, compared to M5, the charge resistance improved for both curing periods due to as the

253 GGBS percentage increases, It forms extra C-S-H gel when it combines with calcium hydroxide.,

254 which fills voids and reduces the porosity of the concrete. This denser microstructure hinders the

255 movement of chloride ions (Kyong and Kyum, 2005).

256 Further tests on M9 to M13 mixes with 2% I-Crete and incremental GGBS additions revealed that

257 the RCPT charge passage for the M11 mix was reduced by 0.37% and 1.35% at 28 and 90 days,

258 respectively, compared to M1. This reduction due to the I-Crete heterogeneous mixture of calcium,

259 silicon, and aluminum oxides, which create a dense pore structure through secondary hydration

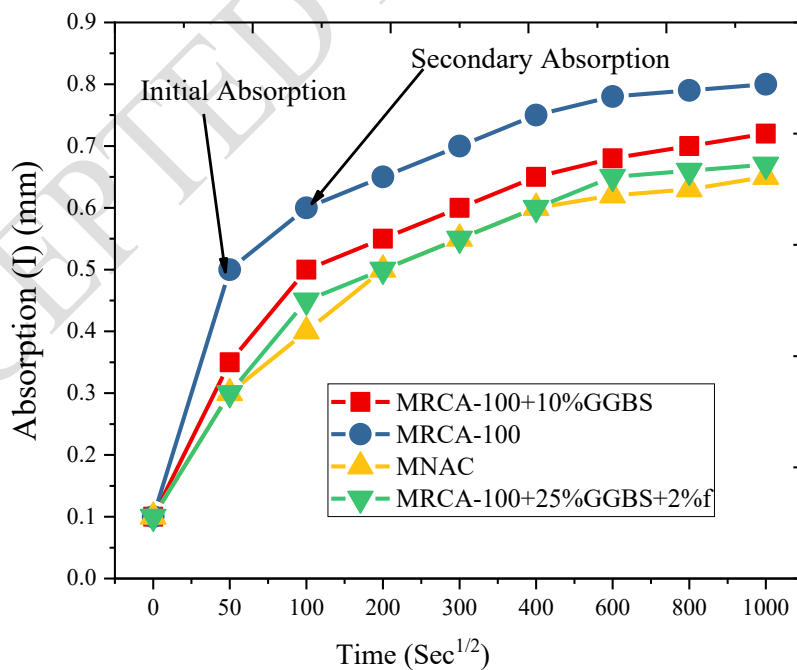
260 reactions beyond just C-S-H gel formation. Additionally, prolonging the curing age significantly

261 reduced charge passage from 28 to 90 days in RA with GGBS composites, as it results in a denser
262 bond at later stages (Jain.J et al.,2012.; Lim et al.,2021), a trend shown in Figure 9.

263 3.4 Sorptivity

264 The Replacement of RA in the control mix M1 leads to an increase in sorptivity. The sorptivity was
265 higher in M5 mix in both primary and secondary observations at 28 days of curing as comparison to
266 M1 mix. RA content, adherent mortar and weak ITZ structure, contribute to this increase. Similar
267 trends have been observed by other researchers, indicating that as RA increases, sorptivity also
268 increases (Kanellopoulos et al., 2014; Olorunsogo and Padayachee,et al., 2002).

269 When GGBS was added up to 10% in the M7 mix, the sorptivity coefficient decreased. The M7 mix
270 achieved optimum strength with GGBS because the ultra-fine particles of GGBS filled the voids,
271 densified the microstructure, increased homogeneity, and promoted C-S-H gel formation. The
272 improved binding and refined pore structure resulted in reduced sorptivity, although it remained
273 higher at 28 days than in the M1 mix (Rama Krishna et al., 2021; Majhi and Naik, 2019; Jindal and
274 Ranginchang, 2017).



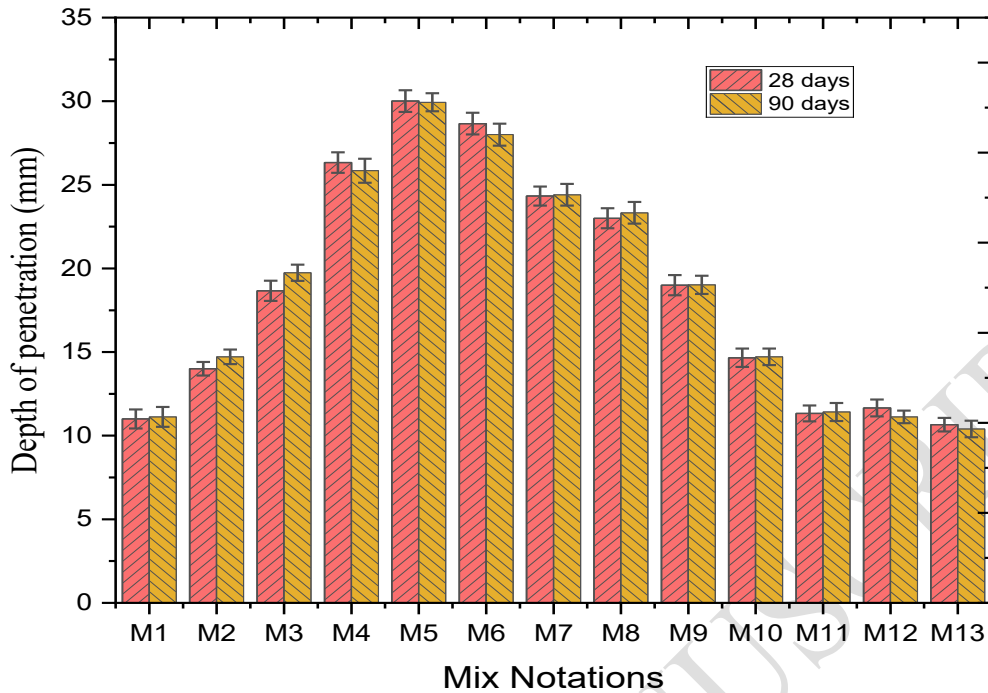
275

276 **Figure 10** Variation of Absorption with Vs Time ($\sqrt{\text{Sec}}$) for all four mixes at 28 days curing period

277 Addition of I-Crete from M9 to M13 revealed that M11 mix exhibited significant reduction in
278 sorptivity with a lower value than M1 mix. I-Crete acts as a highly reactive blended material,
279 forming a dense structure by filling voids and undergoing secondary reactions beyond the formation
280 of a C-S-H gel. The reduction in sorptivity coefficient in the M11 mix highlights the beneficial
281 impact of mineral admixtures on performance of concrete pavements. As curing periods increase,
282 Sorptivity decreases with extended curing as a denser structure forms, and GGBS's low heat of
283 hydration aids bond formation in later stages and For all four optimum mixes, durability and
284 sorptivity classes are rated as good to excellent, measured in absorbance $\text{mm/hr}^{0.5}$ according to
285 source classification (Krishna et al., 2021), as the result are shown in Figure 10.

286 *3.5 Water depth penetration of water under pressure*

287 The depth of water penetration increases with the percentage of incorporated RA up to M5 mix,
288 where the value of penetration at 28 days for M5 mix is 30 mm. According to DIN 1048 and source
289 data from (Krishna et al.,2021) this represents an intermediate classification. For the M5 mix,
290 examined to the M1 mix, the penetration depth increases by 2.72 and 2.69 times at 28 and 90 days
291 of curing, respectively. However, the total water permeability values were low for all the mixes
292 except M5 mix. This increase in penetration can be attached to the pore structure, weak ITZ and
293 mortar adhering to the aggregate (Thomas et al., 2013; Zega et al., 2014).



294

295 **Figure 11** Variation of Depth of penetration with different curing periods for different mixes

296 In M7 mix containing optimum ratio of GGBS and RA, compared to M1, the penetration depth was
 297 2.21 and 2.19 times higher at 28 and 90 days, respectively. However, it shows better penetration
 298 depth compared to M5. This decrease is due to the fine particles of GGBS, which generate less heat
 299 during hydration and contribute to the creation of C-S-H gel, filling the microstructure (Majhi and
 300 Naik, 2019). The addition 2% of I-Crete in mixes M9 to M13, especially mix M11, This led to a
 301 noticeable decrease in penetration depth by 1.03 and 1.02 times at 28 and 90 days of curing,
 302 respectively, examined to M1. The M11 mix performed better than the control mix. I-Crete
 303 improves the bonding structure and helps to form extra bonds than C-S-H gel, making the structure
 304 denser. As the concrete ages and undergoes curing, the penetration depth decreases (Thomas et al.,
 305 2013; Zega et al., 2014). This trend is illustrated in Figure 11.

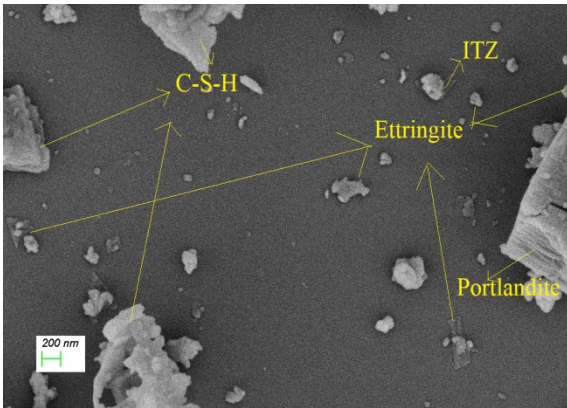
306 4. Morphological analysis

307 4.1. Scanning Electron Microscopic (SEM) Analysis

308 SEM is a popular technique for examining the microstructure of solids, providing high-resolution
 309 images that reveal object shapes and variations in chemical composition, as per the guidelines of

310 Designation: C1723 - 10. SEM was used to study the fracture surfaces of RA with different mineral
 311 contents, focusing on samples cured for 28 days. Figure 12 (a) illustrates the microstructure of M1.
 312 mix at the virgin aggregate-cement interface, highlighting the presence of C-S-H gel and hydroxide
 313 compounds. In contrast, Figure 12 (b) depicts the M5 mix, which differs from ordinary concrete due
 314 to the mortar adhering from the old cement matrix, leading to the creation of two distinct ITZs. The
 315 M5 mix shows abundant needle-like and hexagonal ettringite, as well as more Portlandite calcium
 316 hydroxide particles. This mix also exhibits excess calcium hydroxide with incomplete hydration,
 317 voids, and a weak ITZ. This weak ITZ, due to the loosely bonded mortar, disrupts the aggregate
 318 bond, reducing overall strength (Bonifazi et al., 2015; Ahmad et al., 2022).

319



320

321 Fig.12 (a) MNAC (M1) Mix

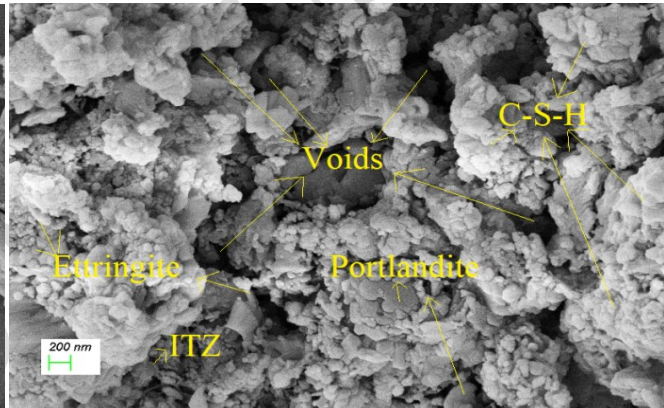
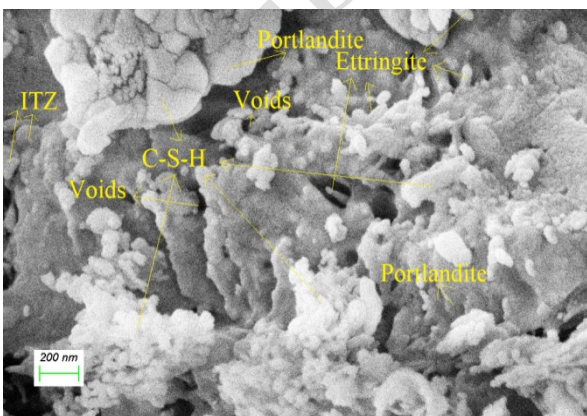
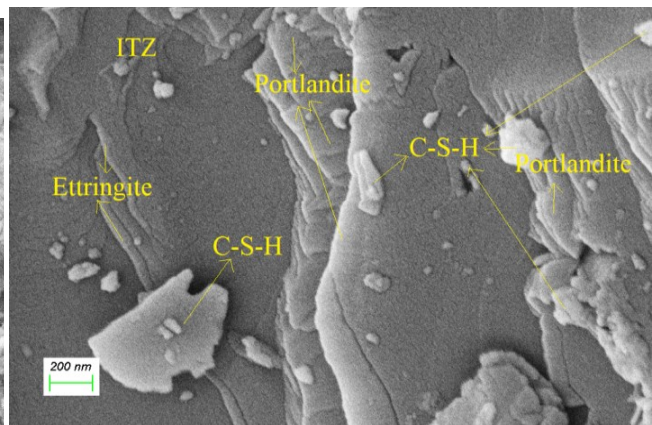


Fig.12 (b) MRCA-100(M5) Mix

322



323 Figure 12 (c) MRCA-100+10%GGBS (M7) Mix



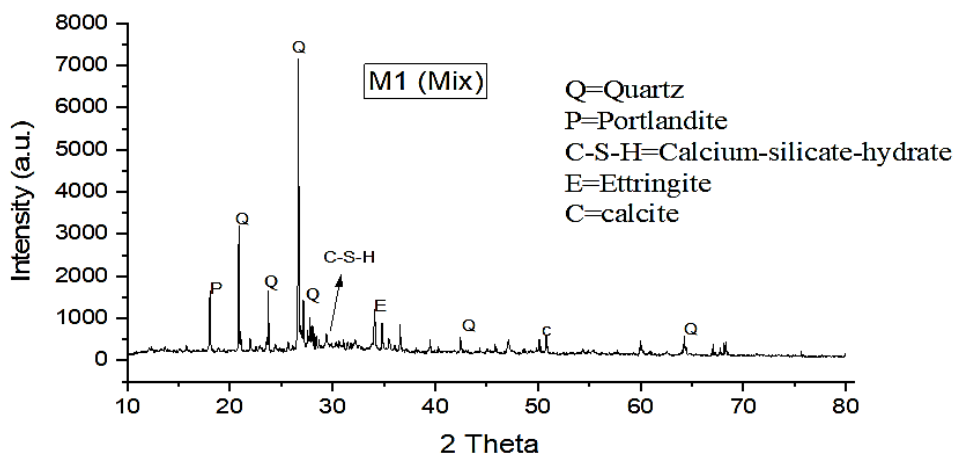
324

Fig.12 (d) MRCA-100+25%GGBS+2I (M11) Mix

325 Figure 12(c) shows the M7 mix, revealing finer GGBS particles, which improve the creation of C-
326 S-H gel, fill the gaps in voids and ITZ, enhance packing efficiency, reduce voids, and distribute
327 stress more evenly. The smooth surfaces and improved workability of these particles contribute to
328 strong ITZ bonding. Previous studies have shown that pozzolanic materials and chemical
329 admixtures can increase ITZ density by producing secondary C-S-H gel, thereby improving the
330 structural integrity of RA with GGBS (Ahmad et al., 2022). Figure 12 (d) illustrates the M11 mix,
331 which contains 25% GGBS and 2% I-Crete. The mixture exhibits elevated levels of C-S-H and
332 calcium hydroxide (CH), accelerating hydration and producing more hydration products, including
333 ettringite. This results in improved compressive strength and durability, particularly beneficial for
334 hard pavement applications, due to reduced voids and enhanced durability.

335 4.2. X-ray diffraction (XRD) Analysis

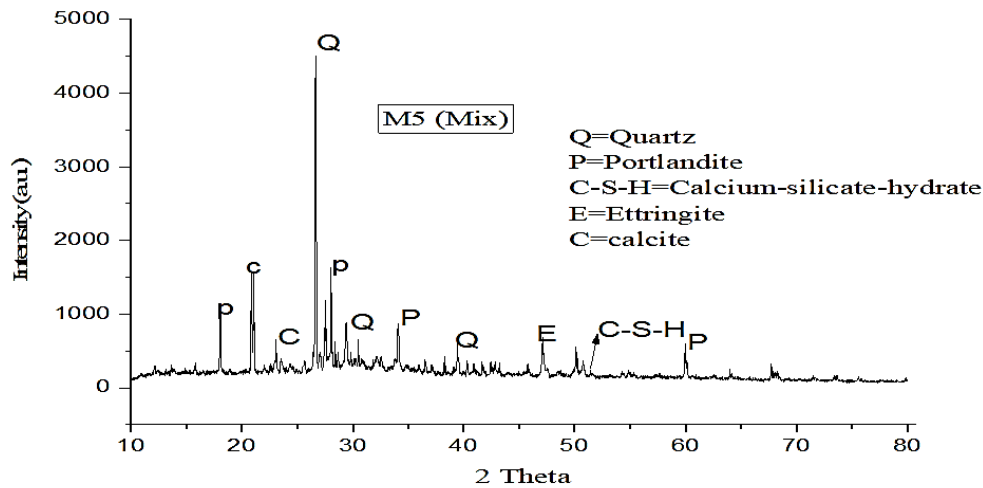
336 X-ray diffraction (XRD) analysis was performed using X'Pert High Score and OriginPro software to
337 determine the chemical composition of the concrete mixtures with 2θ degrees on the x-axis and
338 intensity in arbitrary units (a.u.) on the y-axis. Fig. 13(a) M1 exhibits a mixture with sharp peaks of
339 quartz, ettringite, C-S-H and calcite, Portlandite all of which contribute to strength and energy
340 development. (Majhi & Naik, 2019; Krishna et al., 2021). Portlandite peaks confirm the presence of
341 calcium hydroxide.



342

343 **Figure 13(a)** X-ray diffraction (XRD) diffractogram of the M1 concrete mix

344 Fig. 13(b) Replacement of 100% NA with RA (M5 mix) slightly increases the ettringite and quartz
 345 intensities, while decreasing the C-S-H intensities. The M5 mix exhibits stable ettringite and quartz
 346 peaks, but portlandite intensity increases significantly due to hydrated cement in RA, resulting in
 347 higher calcium hydroxide content and voids (Wang et al., 2020).

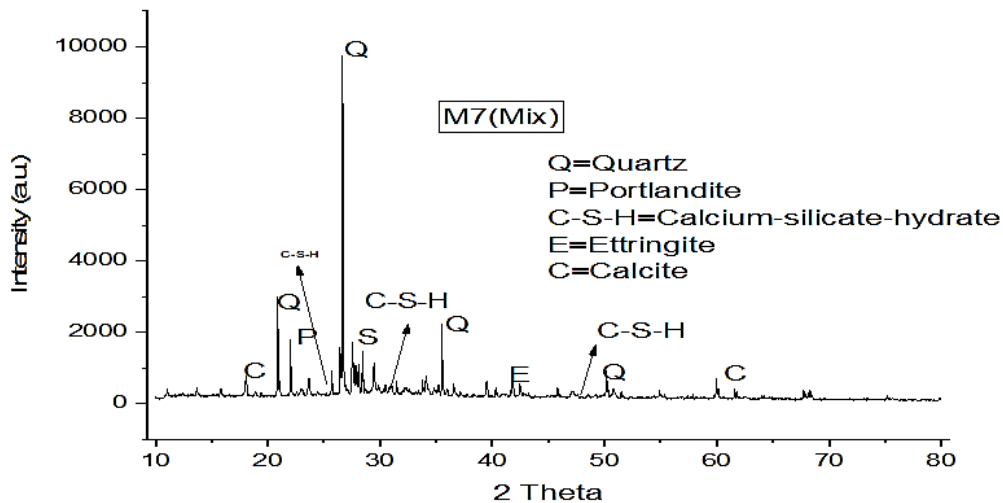


348

349 **Figure 13(b)** X-ray diffraction (XRD) diffractogram of the M5 concrete mix

350 Fig. 13(c) GGBS, which contains more silica than OPC, has been shown to increase quartz and
 351 calcium carbonate, increasing the durability of M7. GGBS reduces the creation of C-S-H and
 352 ettringite, but its pozzolanic reaction weakens portlandite peaks by consuming calcium hydroxide.

353 Fig. 13(d) M11 shows that the mix contains more silica, quartz and ettringite, C-S-H gel, calcite
 354 which increases strength. However, increasing RA content increases calcium hydroxide levels,
 355 leading to higher porosity at the RA-mortar interface.



356

357

Figure 13(c) X-ray diffraction (XRD) diffractogram of the M7 concrete mix

358

Addition of GGBS and I-Crete to RA reduces the formation of ettringite and C-S-H, further

359

reducing strength. However, the pozzolanic reaction of GGBS with amorphous silica consumes

360

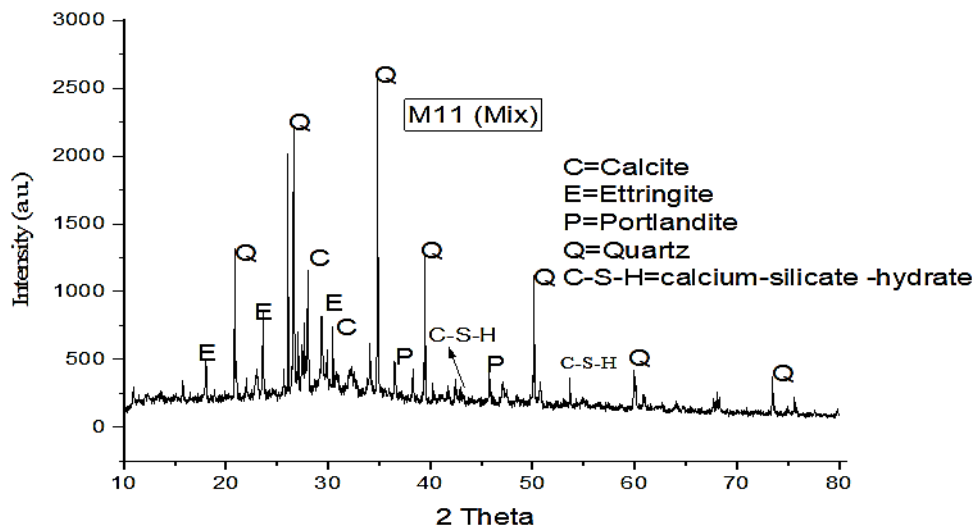
calcium hydroxide, improving durability. Increased crystalline silica and calcium carbonate

361

formation further enhances the filling effect, increasing the durability of RA with GGBS and I-

362

Crete.



363

Figure 13(d) X-ray diffraction (XRD) diffractogram of the M11 concrete mix

364

365 5. Conclusion

366

The findings of this study have important practical implications for large-scale pavement

367

applications, especially in terms of sustainability and durability. The use of RA in combination with

368

additives like GGBS and I-Crete can reduce material costs, conserve natural resources, and improve

369

the performance of concrete in pavements. The study demonstrates that with proper mix design and

370

the incorporation of durability-enhancing additives, high RA content in PQC can lead to durable,

371

cost-effective, and environmentally friendly pavements, making it a viable option for large-scale

372

infrastructure projects. The findings of this research are

373

1. The PQC of M40 mix had a compressive strength of 51.20 MPa and 52.81 MPa at 28 and 90

374

days for M1 mix. The replacement of 100% NA with RA in the M5 mix reduced the compressive

375

strength by 5.66% and 5.60% at 28 and 90 days, respectively, due to higher voids and weaker ITZ

376 from the adhered mortar. When 10% of cement in M5 was replaced with GGBS in M7 mix, the
377 compressive strength decreased by 4.68% and 4.75% compared to M1, but improved over M5 mix.
378 This improvement is due to the fine particles of GGBS filling the voids and creating a dense
379 structure. Replacing cement with 25% GGBS and adding 2% I-Crete to the M11 mix slightly
380 increased the compressive strength by 0.19% and 0.185% compared to M1, demonstrating that I-
381 Crete provides a sustainable alternative without compromising strength.

382 2. M1 mixture exhibited drying shrinkage strains of 9.63×10^{-5} (%) and 15.40×10^{-5} (%) at 28
383 and 90 days. The M5 mix had 4.92 times greater strains at 28 days and 3.71 times greater strains at
384 90 days – due to increased porosity and weaker ITZ from RA. M7 mix showed 3.64 and 2.60 times
385 more reduced strains than M1 at 28 and 90 days, indicating better performance. M11 mix with I-
386 crete showed even better stability with 1.89 and 1.31 times higher strains respectively, than M1,
387 reflecting improved performance while maintaining strength.

388 3. The RCPT charge is 385.55 and 375.2 coulombs for M1 at 28 and 90 days, accordingly. In the
389 M5 mix, due to the higher void content, the charge increased by 97.37% and 89.21% compared to
390 M1. M7 showed an improvement of the mix, the charge increased by 60.95% and 59.89%
391 compared to M1, to the filling of GGBS vacancies and the formation of C-S-H gel. M11 mixture
392 showed a slight decrease in charge passage of 0.37% and 1.37% compared to M1, attributed to the
393 improved bonding and secondary reactions of I-Crete, highlighting the role of admixtures in
394 improving concrete durability.

395 4. M1 mix has better water absorption (Sorptivity) resistance at 28 days. However, replacement of
396 NA with RA in the M5 mixture resulted in higher absorption due to increased voids. M7 mix, with
397 10% GGBS, showed better resistance compared to M5, but less than M1 because GGBS reduces
398 voids. Supplementation with 25% GGBS and addition of 2% I-Crete in M11 led to even lower
399 absorption overtaking M1. This improvement is due to I-Crete improving bond strength,
400 demonstrating an inverse Relationship among water absorption and compressive strength.

401 5. The depth of water penetration for M1 was 11 mm and 10.33 mm at 28 and 90 days. The
402 penetration depth increased with 100% RA in M5 mixture, reaching 30 mm and 27.80 mm at 28
403 and 90 days, respectively. It is 2.72 and 2.69 times higher than M1. Adding GGBS to RA reduced
404 the penetration by 2.21 and 2.19 times, while adding I-Crete with 25% GGBS in M11 reduced it by
405 1.03 and 1.02 times compared to M1. These compounds improve durability, making the mixture
406 suitable for sustainable pavement construction.

407 6. SEM analysis shows that GGBS and I-Crete significantly improve the ITZ of RAC by improving
408 particle packing, reducing voids and increasing C-S-H content. This leads to higher compressive
409 strength and durability, especially for hard pavement applications, compared to mixes with weak
410 ITZ due to stuck mortar and incomplete hydration.

411 7. XRD analysis concludes that incorporating GGBS into RAC significantly enhances durability by
412 consuming excess calcium hydroxide and refining the microstructure. However, increased RCA
413 content reduces concrete strength due to increased porosity at the RCA-mortar interface. The M11
414 mix, with higher GGBS content, exhibits superior strength and durability, making it an ideal choice
415 for sustainable construction.

416 Substituting Natural Aggregates (NA) with Recycled Aggregates (RA) has significant
417 environmental benefits, primarily in reducing the demand for virgin resources and minimizing the
418 environmental impact of quarrying. The use of RA in pavement concrete not only helps in recycling
419 construction and demolition waste but also reduces the carbon footprint associated with extracting
420 and processing NA. The study suggests that higher RA content in PQC mixes could contribute to
421 sustainable pavement construction by reducing landfill waste, conserving natural resources, and
422 lowering greenhouse gas emissions.

423 **Future Recommendations**

424 Future studies should explore the long-term performance of RAC with different GGBS and I-Crete
425 ratios, focusing on freeze-thaw resistance, fatigue behavior, and life-cycle cost analysis to further
426 validate their use in sustainable pavement construction.

427 **Acknowledgement**

428 The authors thank Sri Vishnu Sai Saravana Enterprises, Visakhapatnam, for supplying GGBS,
429 Navodya Private Limited, Chennai, for providing I-Crete, and the C&D Waste Plant, Hyderabad,
430 for delivering recycled aggregate. We also thank Andhra University, Visakhapatnam, for providing
431 laboratory facilities.

432 **Reference**

433 Ahmad, J., Kontoleon, K. J., Majdi, A., Naqash, M. T., Deifalla, A. F., Ben Kahla, N., ... & Qaidi,
434 S. M. (2022). A comprehensive review on the ground granulated blast furnace slag (GGBS) in
435 concrete production. *Sustainability*, **14**(14), 8783.

436 Bonifazi, G., Capobianco, G., Serranti, S., Eggimann, M., Wagner, E., Di Maio, F., & Lotfi, S.
437 (2015). The ITZ in concrete with natural and recycled aggregates: Study of microstructures based
438 on image and SEM analysis. *Proc. 15th Euroseminar Microsc. Appl. to Build. Mater*, 299-308.

439 Designation: C 1585 – 04 Standard Test Method for Measurement of Rate of Absorption of Water
440 by Hydraulic Cement Concretes¹.

441 Designation: C1202 – 12 Standard Test Method for Electrical Indication of Concrete's Ability to
442 Resist Chloride Ion Penetration¹.

443 Designation: C192/C192M – 18 C192/C192M – 19 Standard Practice for Making and Curing
444 Concrete Test Specimens in the Laboratory¹.

445 Designation: C1723 – 10 Standard Guide for Examination of Hardened Concrete Using Scanning
446 Electron Microscopy¹.

447 Duan, Z. H., & Poon, C. S. (2014). Properties of recycled aggregate concrete made with recycled
448 aggregates with different amounts of old adhered mortars. *Materials & Design*, **58**, 19-29.

449 Hwang, J. P., Shim, H. B., Lim, S., & Ann, K. Y. (2013). Enhancing the durability properties of
450 concrete containing recycled aggregate by the use of pozzolanic materials. *KSCE Journal of Civil
451 Engineering*, **17**, 155-163.

452 <https://www.ecomaterials.in/products-i-crete.php>

453 IRC:44-2017: Guidelines for Cement Concrete mix Design for pavements.

454 IRC:121-2017: Guidelines for use of Construction and Demolition Waste in road sector.

455 IS516(Part2/sec1): 2018 determination of depth of penetration of water under pressure.

456 IS516(Part6):2020 Determination of drying shrinkage of concrete and moisture movement of
457 concrete samples

458 IS2645:2005 Indian Standard integral waterproofing compounds for cement mortar and concrete—
459 specification

460 IS 1199: Part 2 : 2018: Fresh Concrete— Methods of Sampling, Testing and Analysis Part 2
461 Determination of Consistency of Fresh Concrete (First Revision)

462 IS 2514: Specification for concrete vibrating tables.

463 IS 12089: Specification for granulated slag for the manufacture of Portland slag cement

464 IS. 456 : 2000 Indian Standard Plain and Reinforced Concrete - Code of practice.

465 IRC:15-2017 Code of practice for construction of jointed plain concrete pavements.

466 IS 10262 : 2019: Concrete Mix Proportioning — Guidelines .

467 IS383:2016 Coarse and fine aggregate for concrete-Specification.

468 IS 516 : Part 1 : Sec 1 : 2021: Hardened concrete methods of test part 1 testing of strength of
469 hardened concrete section 1 compressive, flexural and split tensile strength.

470 Jain, J., Verian, K. P., Olek, J., & Whiting, N. (2012). Durability of pavement concretes made with
471 recycled concrete aggregates. *Transportation research record*, 2290(1), 44-51.

472 Jindal, A., Ransinchung RN, G. D., & Kumar, P. (2017). Study of pavement quality concrete mix
473 incorporating beneficiated recycled concrete aggregates. *Road Materials and Pavement
474 Design*, **18(5)**, 1159-1189.

475 Jindal, A. (2016). Durability studies of PQC mix incorporating recycled concrete aggregate and
476 mineral admixtures.

477 Kanellopoulos, A., Nicolaidis, D., & Petrou, M. F. (2014). Mechanical and durability properties of
478 concretes containing recycled lime powder and recycled aggregates. *Construction and Building*
479 *Materials*, **53**, 253-259.

480 Kou, S. C., Poon, C. S., & Agrela, F. (2011). Comparisons of natural and recycled aggregate
481 concretes prepared with the addition of different mineral admixtures. *Cement and Concrete*
482 *Composites*, **33(8)**, 788-795.

483 Krishna, N. R., Rao, A. S., & Sasidhar, C. (2021, April). Experimental Investigations On
484 Mechanical And Durability Properties Of Blended Concrete. In *IOP Conference Series: Materials*
485 *Science and Engineering* (Vol. 1130, No. 1, p. 012036). IOP Publishing.

486 Kumar, A., & Singh, G. J. (2023). Improving the physical and mechanical properties of recycled
487 concrete aggregate: A state-of-the-art review. *Engineering Research Express*, **5(1)**, 012007.

488 Kumar, G., & Mishra, S. S. (2022). Effect of recycled concrete aggregate on mechanical, physical
489 and durability properties of GGBS–fly ash-based geopolymer concrete. *Innovative Infrastructure*
490 *Solutions*, **7(4)**, 237.

491 Lim, Y. Y., & Pham, T. M. (2021). Effective utilisation of ultrafine slag to improve mechanical and
492 durability properties of recycled aggregates geopolymer concrete. *Cleaner Engineering and*
493 *Technology*, **5**, 100330.

494 Majhi, R. K., & Nayak, A. N. (2019). Bond, durability and microstructural characteristics of ground
495 granulated blast furnace slag based recycled aggregate concrete. *Construction and Building*
496 *Materials*, **212**, 578-595.

497 Mao, Y., Liu, J., & Shi, C. (2021). Autogenous shrinkage and drying shrinkage of recycled
498 aggregate concrete: A review. *Journal of Cleaner Production*, **295**, 126435.

499 Ministry of Road Transport and Highways (MORTH) Standards.

500 Nandanam, K., Biswal, U. S., & Dinakar, P. (2021). Effect of fly ash, GGBS, and metakaolin on
501 mechanical and durability properties of self-compacting concrete made with 100% coarse recycled
502 aggregate. *Journal of Hazardous, Toxic, and Radioactive Waste*, **25(2)**, 04021002.

503 Olorunsogo, F. T., & Padayachee, N. (2002). Performance of recycled aggregate concrete
504 monitored by durability indexes. *Cement and concrete research*, **32**(2), 179-185.

505 Sarma, V. V. S., Subhan Alisha, S., Vijay, K., Gireesh Kumar, P., & Sai Kumar, K. S. (2024).
506 Mechanical performance enhancement of recycled aggregate concrete using GGBS and fly ash for
507 sustainable construction. *Multiscale and Multidisciplinary Modeling, Experiments and Design*, **7**(3),
508 1693-1700.

509 Sharma, P., Verma, M., & Sharma, N. (2021, April). Examine the mechanical properties of recycled
510 coarse aggregate with MK GGBS. In *IOP conference series: materials science and
511 engineering* (Vol. 1116, No. 1, p. 012152). IOP Publishing.

512 Silva, R. V., De Brito, J., & Dhir, R. K. (2019). Use of recycled aggregates arising from
513 construction and demolition waste in new construction applications. *Journal of Cleaner
514 Production*, **236**, 117629.

515 Singh, Y., & Singh, H. (2021). Recycling Construction and Demolition Waste: Potential
516 Applications and the Indian Scenario. In *Integrated Approaches Towards Solid Waste
517 Management* (pp. 273-281). Cham: Springer International Publishing.

518 Tam, V. W., Soomro, M., & Evangelista, A. C. J. (2018). A review of recycled aggregate in
519 concrete applications (2000–2017). *Construction and Building materials*, **172**, 272-292.

520 Teng, S., Lim, T. Y. D., & Divsholi, B. S. (2013). Durability and mechanical properties of high
521 strength concrete incorporating ultra fine ground granulated blast-furnace slag. *Construction and
522 Building Materials*, **40**, 875-881.

523 Thomas, C., Setién, J., Polanco, J., Alaejos, P., & De Juan, M. S. (2013). Durability of recycled
524 aggregate concrete. *Construction and building materials*, **40**, 1054-1065.

525 Wang, B., Yan, L., Fu, Q., & Kasal, B. (2021). A comprehensive review on recycled aggregate and
526 recycled aggregate concrete. *Resources, Conservation and Recycling*, **171**, 105565

527 Wang, J., Xie, J., Wang, C., Zhao, J., Liu, F., & Fang, C. (2020). Study on the optimum initial
528 curing condition for fly ash and GGBS based geopolymer recycled aggregate
529 concrete. *Construction and Building Materials*, **247**, 118540.

530 Yeau, K. Y., & Kim, E. K. (2005). An experimental study on corrosion resistance of concrete with
531 ground granulates blast-furnace slag. *Cement and Concrete Research*, **35(7)**, 1391-1399.

532 Yu, Y., Wang, P., Yu, Z., Yue, G., Wang, L., Guo, Y., & Li, Q. (2021). Study on the effect of
533 recycled coarse aggregate on the shrinkage performance of green recycled
534 concrete. *Sustainability*, **13(23)**, 13200.

535 Zega, C. J., Di Maio, Á. A., & Zerbino, R. L. (2014). Influence of natural coarse aggregate type on
536 the transport properties of recycled concrete. *Journal of materials in civil engineering*, **26(6)**,
537 04014006.

538 Zhang, P., Sun, X., Wang, F., & Wang, J. (2023). Mechanical properties and durability of
539 geopolymer recycled aggregate concrete: A review. *Polymers*, **15(3)**, 615.

540 Zhang, W., Hama, Y., & Na, S. H. (2015). Drying shrinkage and microstructure characteristics of
541 mortar incorporating ground granulated blast furnace slag and shrinkage reducing
542 admixture. *Construction and building materials*, **93**, 267-277.

543 Zhang, W., Zakaria, M., & Hama, Y. (2013). Influence of aggregate materials characteristics on the
544 drying shrinkage properties of mortar and concrete. *Construction and building materials*, **49**, 500-
545 510.

546 **Response to Reviewer and Editor Comments:**

REVIEWER (I)	Authors	Amended text
Why 2% of I-crete was chosen is not mentioned. can place error bars on all the test results represented in graphs.	The reason for choosing 2% I-crete is mentioned. The error bars are placed on all the applicable graphs.	The reason for 2% I-Crete was added in section 2.1 under data collection in the last paragraph and highlighted in green color. Additionally,

		error bars have been implemented in Figures 7, 8, 9, and 11.
Can improve the writing language and can improve the graph's quality and presentation.	The writing language and the quality of the graphs were enhanced for better presentation	The writing language The quality of the graphs in Figures 1 to 12 has been improved to the best possible standard. highlighted in green color
REVIEWER (D)		
Are the references correctly written? its not in as per guideline	References have been revised to comply with the specified guidelines.	References have been revised
Does the Graphical Abstract correspond the central idea of the paper? not matched	The Graphical Abstract has been revised to align with the central idea of the paper	The graphical abstract has been revised and pasted in the revised manuscript.
1. Provide a clearer rationale for selecting the specific RA replacement percentages and their potential impact on performance.	Recycled aggregate (RA) replacement percentages range from 25% to 100% to assess concrete performance. At lower RA levels, the impact is minimal, while higher levels significantly affect concrete behavior..	The rationale for selecting the specific RA replacement percentages and their potential impact on performance has been discussed in the last paragraph of section 3.1 under compressive strength and highlighted in blue color.
2. Elaborate on the	Compared to the traditional	The reasons have been added

significance of I-Crete addition for durability enhancement compared to traditional additives.	additives, I-Crete, with its lower dosage, enhanced the durability behavior.	and discussed in the last paragraph of section 2.3 and highlighted in blue color.
3. Include more statistical analysis to support the compressive strength results across different mixes.	Statistical analysis, such as standard deviation, is performed on each mix, and it is presented as error bars on the respective graphs.	Statistical analysis, such as standard deviation, was performed on each mix and presented as error bars on the respective graphs. This is discussed below Figure 7 and highlighted in blue color.
4. Provide additional explanation for how drying shrinkage is impacted by higher RA levels.	Parameters such as higher water demand, higher porosity, and weaker Interfacial Transition Zone affect drying shrinkage at higher RA levels.	Additional explanation on how drying shrinkage is impacted by higher RA levels has been added in section 3.2 and highlighted in blue color.
5. Check for grammatical errors throughout the manuscript to improve readability.	Yes, the grammatical errors were rectified.	Yes, the grammatical errors have been rectified and highlighted in blue color.
6. Ensure all formatting adheres to the journal's guidelines, particularly in the tables and figures.	The article is properly aligned with the journal guidelines.	Yes, all possible formatting has been adjusted to adhere to the journal's guidelines, particularly in the tables and

		figures, and highlighted in blue color.
7. Clarify the methodology used for measuring water penetration and RCPT values in all tested samples.	The water penetration depth was measured according to IS:516:part2:sec1:2018 while the RCPT was conducted following ASTM C1202, with the total charge passed through 50-mm thick discs subjected to a 60 V DC current for 6 hours to assess chloride ion penetration.	The water penetration depth was measured as per IS:516:Part 2:Sec 1:2018, and the RCPT was conducted following ASTM C1202. This is added in section 3.3 and highlighted in blue color in the first paragraph.
8. Verify the accuracy of all units presented in tables, especially in the compressive strength and shrinkage data.	The accuracy of all the units is rectified, and necessary changes are incorporated.	The accuracy of all the units is rectified.
9. Include a discussion on the environmental impact of substituting NA with RA in pavement concrete.	Discussion is added.	A discussion on the environmental impact of substituting natural aggregates (NA) with recycled aggregates (RA) in pavement concrete has been added after the conclusion and highlighted in blue color.
10. Specify the testing standards followed for each	The codes of conduct for sorptivity and RCPT were	The testing standards followed for each durability parameter,

durability parameter, such as sorptivity and RCPT.	ASTM-C-1202 and ASTM-C-1585-04.	such as sorptivity and RCPT, have been specified in section 2.2 under data measurement and highlighted in blue color.
11. Improve the clarity of technical terms, ensuring all abbreviations are defined on first use.	The suggestions are considered, and all the abbreviations are mentioned in their first use.	All technical terms and abbreviations have been clarified, with definitions provided on first use in the abstract, in Table 1, and at the beginning of paragraphs for new technical terms.
12. Provide a comparison of the drying shrinkage behavior of each mix with other studies in similar domains.	The revised manuscript now includes a comparative analysis of drying shrinkage behavior across mixes, highlighting reduced shrinkage with recycled aggregates, GGBS, and I-Crete in line with similar studies.	A comparison of the drying shrinkage behavior of each mix with other studies in similar domains has been discussed in section 3.2 below Figure 8 and highlighted in blue color.
13. Elaborate on how GGBS and I-Crete combine to counteract the reduction in compressive strength with higher RA content.	The elaboration of how GGBS and I-Crete counteract the reduction in compressive strength is mentioned in the manuscript.	An explanation of how GGBS and I-Crete work together to counteract the reduction in compressive strength with higher RA content has been added above Figure 8 and

		highlighted in blue color.
14. Highlight the practical implications of this research for large-scale pavement applications.	Yes, the practical implications of applications are added in the manuscript.	The practical implications of this research for large-scale pavement applications have been discussed and added to the beginning of the conclusion, highlighted in blue color.
15. Conduct a spell check as some terms have minor spelling errors, affecting the manuscript's professionalism.	The spell check is done.	A spell check has been completed in the revised manuscript.
ASSOCIATE EDITOR (A)		
Barely the environmental implications of the replacement must be better discussed	the revised manuscript now includes an expanded discussion on the environmental implications of material replacements, highlighting their benefits for sustainability and carbon footprint reduction	The environmental implications of the replacement have been discussed below the conclusion and highlighted in blue color.
Graphical Abstract, novelty of the paper, Are figures and tables, Methods, paper's contribution significant	the revised manuscript now incorporates all suggested improvements, including an updated Graphical Abstract, a	As per the reviewer's suggestion, the graphical abstract, novelty of the paper, significance of figures and

	clear statement of the paper's novelty, enhanced figures and tables, refined methods, and a more detailed explanation of the paper's contribution, ensuring alignment with the reviewer's recommendations.	tables, methods, and the paper's contribution have been discussed in the revised manuscript.
--	--	--

547

ACCEPTED MANUSCRIPT